Refraction control of acoustic waves in a square-rod-constructed tunable sonic crystal

Liang Feng,[1] Xiao-Ping Liu,[1] Ming-Hui Lu,[1] Yan-Bin Chen,[2] Yan-Feng Chen,[1,*] Yi-Wei Mao,[3] Jian Zi,[4] Yong-Yuan Zhu,[1] Shi-Ning Zhu,[1] and Nai-Ben Ming[1]

[1]*National Laboratory of Solid State Microstructures and Department of Materials Science and Engineering, Nanjing University, Nanjing 210093, People's Republic of China*

[2]*Department of Materials Science and Engineering, University of Michigan, Ann Arbor, Michigan 48109, USA*

[3]*Institute of Acoustics, Nanjing University, Nanjing 210093, People's Republic of China*

[4]*National Laboratory of Surface Physics, Fudan University, Shanghai 200433, People's Republic of China*

(Received 9 November 2005; revised manuscript received 8 February 2006; published 3 May 2006)

A two-dimensional square-rod-based tunable sonic crystal was constructed by 1.6 mm-wide steel square rods in air with a lattice constant of 2.5 mm to operate in an ultrasonic regime. By means of simply rotating square rods, the scattering sections, corresponding to different geometric factors of the sonic crystal, have been changed to manipulate the refraction from positive to negative, and thus produce a tunable acoustic superlens. These results show an effective method to control wave propagations in not only sonic crystals, but also other periodic structures, such as light in photonic crystals and water propagation in periodic rods.

DOI: 10.1103/PhysRevB.73.193101 PACS number(s): 78.20.Ci, 43.35.+d, 63.20.−e

Wave refraction has been a subject of considerable interest. In the common sense, refractions are always positive. Negative refraction of light, however, was first theoretically predicted in left-handed materials (LHM) with both permittivity and permeability simultaneously negative[1] and experimentally observed in two-dimensional (2D) LHM by an array of split-ring resonators and wires.[2–7] Besides LHM, photonic crystals were also proposed, by analyzing PCs by equi-frequency surfaces (EFS),[8–11] to realize the negative refraction in both microwave and infrared regions, which resulted from intense multiple scatterings instead of double negative permittivity and permeability. Based on negative refractions, a kind of flat lens was also proposed and established as a superlens to make use of both evanescent waves and propagating waves to produce a real image beyond the diffraction limit.[11–15] Now, like photonic crystals, negative refraction has gone into acoustics in sonic crystals and other classical waves, also leading to a superlensing effect.[16–20]

It is highly desired to obtain some degrees of tunability in wave refractions. Light refractions could be modulated from positive to negative by altering photonic crystals' permittivity or (and) permeability with applied fields.[21,22] But it is difficult to change analogous parameters, such as the density and modulus in sonic crystals. Can acoustic refractions be tuned from positive to negative? And how large can the tuning range of acoustic refraction reach? In this paper, we will attempt to address these questions in a square-rod-constructed sonic crystal (SRSC) by geometric adjustments.[23–25] To our knowledge, the refraction control is discussed in acoustics and the acoustic tunable superlens is experimentally constructed for the first time, whose very large tuning range will allow great potential applications in light, sound, and liquid wave propagations. In the present experiment, a 2D SRSC was constructed, in which the lattice constant is $a=2.5$ mm and the width of the rods is 1.6 mm, resulting in a filling fraction of approximately 41%.[26]

For the noncircular-structure-based sonic crystal, the multiple scattering method is difficult to be used to calculate the band structure if not impossible. But plane wave expansion method could be well applied to solve this problem.[23–25] Especially in the giant impedance mismatch system like our sonic crystal consisting of air and steel, the sound almost does not penetrate steel cylinders and hence the propagation is confined and predominant only in the air so that only longitude waves are considered in the sonic crystal because there is no shear acoustic wave propagating in air.[27] For the SRSC of square rods of rotational angle θ (see the inset of Fig. 1), the geometric factor $I(\vec{G})$, used to expand every parameter including $\frac{1}{\lambda(r)}$, $\frac{1}{\rho(r)}$ and $u(r)$ in the plane wave expansion, is defined as follows Refs. 23–25:

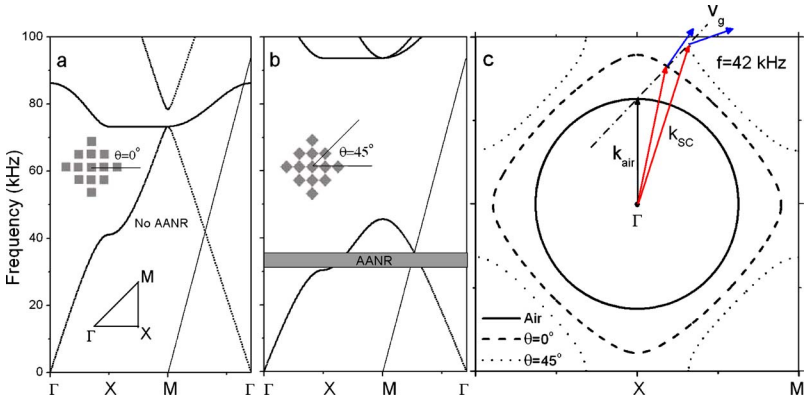

FIG. 1. (Color online) Theoretical demonstration of tunable acoustic negative refraction in SRSC. (a) and (b) are band structures of the SRSC with $\theta=0°$ and $\theta=45°$, respectively. The shaded region in (b) denotes the all angle negative refraction region with the surface normal of Γ-M direction. (c) is EFSs in k space of air (solid) and SRSC with both $\theta=0°$ (dashed) and $\theta=45°$ (dotted) at 42 kHz; v_g is the group velocity in the acoustic crystal.

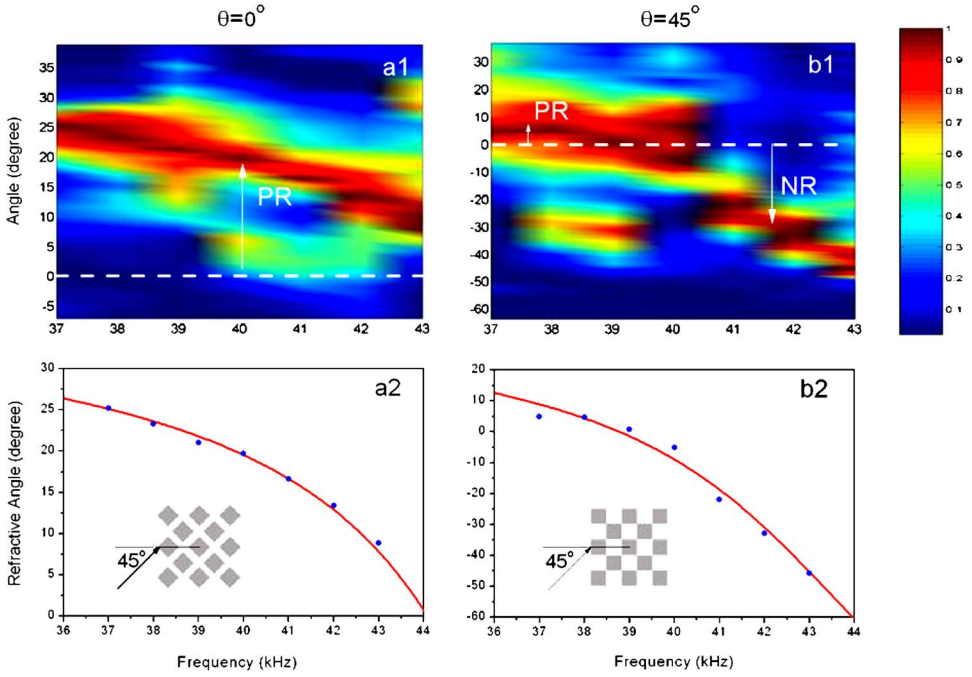

FIG. 2. (Color online) The dependence of tunable refraction on frequencies for the incident angle of 45° with (a) θ=0° and (b) θ =45°, respectively. (a1) and (b1) are the average acoustic transmission intensity versus frequency (kHz) and angle for the SRSC. The refraction was considered negative refraction (NR) or positive refraction (PR) if the maximum transmission intensity is detected at the up or under side of the surface normal, respectively. The average intensity scale varies from 0 to 1. (a2) and (b2) are comparisons of experimental measurements (dots) and theoretical simulations (line) of refractive angles versus frequencies.

$$I(\vec{G}) = F\frac{\sin(\tilde{G}_x l/2)}{\tilde{G}_x l/2}\frac{\sin(\tilde{G}_y l/2)}{\tilde{G}_y l/2}, \quad (1)$$

in which

$$\begin{pmatrix}\tilde{G}_x\\ \tilde{G}_y\end{pmatrix} = \begin{pmatrix}\cos\theta & \sin\theta\\ -\sin\theta & \cos\theta\end{pmatrix}\begin{pmatrix}G_x\\ G_y\end{pmatrix}$$

and F is the filling fraction. Since the filling fraction in our SRSC is only 41%, θ could be rotated from 0° to 45°, and extremely demonstrate its tunablity. There is only a little difference in band structures and refraction angles (less than 1%) between the rotation angle θ and $-\theta$. In this paper, we only show the results of θ from 0° to 45°, which can effectively reveal that our refraction controllable scheme is also available for θ from 0° to −45° since the configuration of θ=45° is totally identical to that of θ=−45°.

The propagation of acoustic waves in sonic crystals is an accumulated effect of multiple scatterings, so it is very sensitive to the scattering section in one unit cell. The scattering section is the effective scattering area of the sonic crystal, which is introduced in Eq. (1) of the geometric factor using

$$\begin{pmatrix}\tilde{G}_x\\ \tilde{G}_y\end{pmatrix} = \begin{pmatrix}\cos\theta & \sin\theta\\ -\sin\theta & \cos\theta\end{pmatrix}\begin{pmatrix}G_x\\ G_y\end{pmatrix}.$$

So corresponding to different rotational angles θ, the scattering sections to acoustic waves in one unit cell are different due to the geometric differences, analog to the case in x-ray scatterings by crystals. Hence, the total effect of multiple scatterings in the SRSC based on the Bloch symmetry will be dramatically changed by rotating the square rods. The SRSCs band structures are calculated with 289 plane waves as shown in Fig. 1. The acoustic band gaps are enlarged gradually by increasing the rotational angle θ from 0° to 45°. For the larger rotational angle, the lowest acoustic band is decreased and compressed, corresponding to more intense anisotropy that could be easily understood through the EFSs shown in Fig. 1(c) where the frequency is 42 kHz. The anisotropy of wave propagation is determined by the curvature of EFS. The more dramatic modification of the EFS corre-

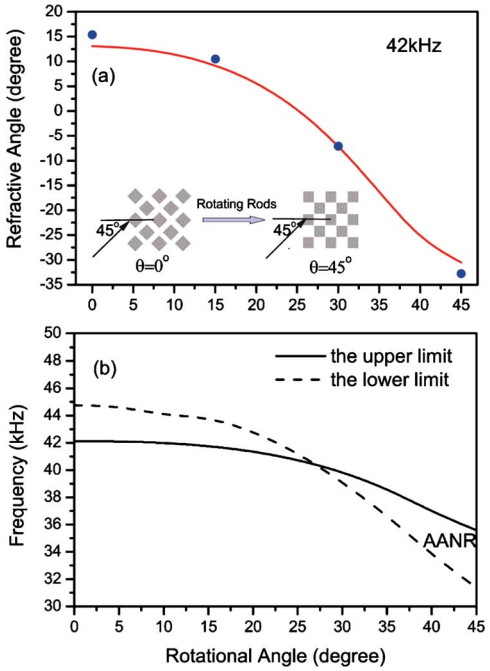

FIG. 3. (Color online) Tunability of the SRSC with rotational angles θ. (a) is the comparison of measured (dots) and calculated (line) angles of refraction versus rotational angles θ at 42 kHz for the incident angle of 45°, demonstrating a tunability for a single beam. (b) is the control of AANR, exhibiting an imaging tunability with a tunable acoustic superlens. AANR occurs only when its upper limit (solid) is higher than its lower limit (dashed).

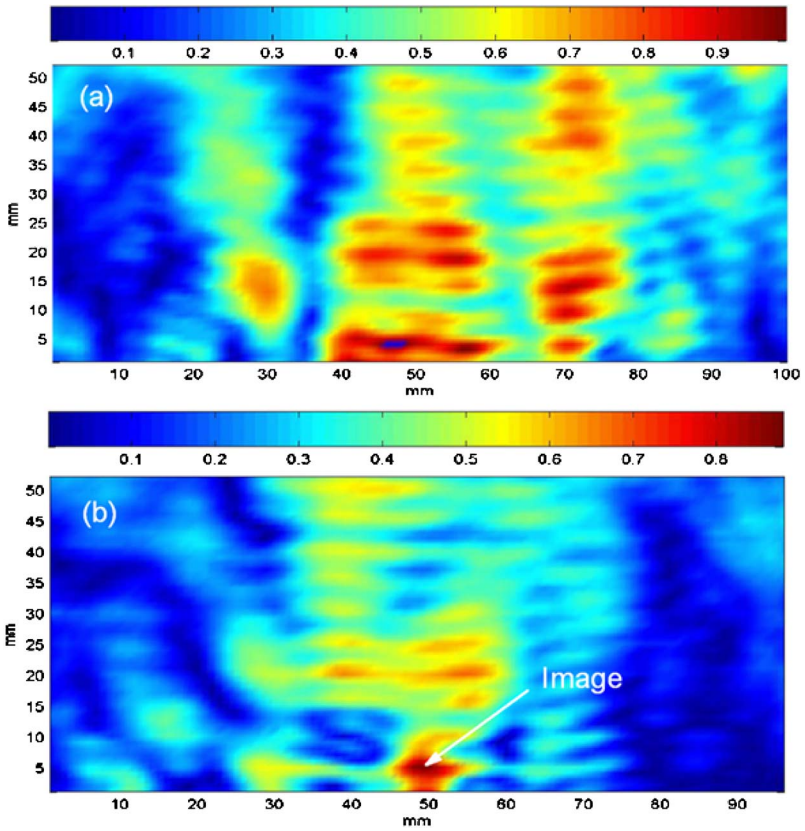

FIG. 4. (Color online) Tunable superlensing effect of the SRSC at 35 kHz. (a) has no image without AANR and (b) is a good image with AANR.

sponds to the greater anisotropy. With increasing θ, the scattering section in one unit will be enlarged as the geometric factor increases, which leads to dramatic modifications of SRSCs EFS and the anisotropy of wave propagation. In comparison with $\theta=0°$, the scattering section is enlarged by a factor of $\sqrt{2}$ when $\theta=45°$ so that the anisotropy of EFS is effectively enhanced.

The anisotropy of EFS determines the propagation and refraction of acoustic waves in SRSC. Due to the sensitivity of anisotropy to the rotational angle θ, the wave refraction also varies with θ. From Fig. 1(c), with the surface normal of SRSC along Γ-M direction ([1, 1] in real space), it is obvious that the great anisotropy at larger rotational angles such as $\theta=45°$ produces negative refraction, while the refraction is positive when the rotational angles are smaller such as $\theta=0°$. So with the supposed parameter of SRSC, rotating θ from 0° to 45° will effectively manipulate the refraction from positive to negative. And the larger the rotational angle θ, the greater the negative refraction angle.

To verify the analysis of the refraction of acoustic waves, a scanning transmission measurement of spatial distributions covering frequencies from 37 to 43 kHz was carried out by various rotational angles with the incidence of 45°. The experimental setup is the same as our previous paper.[19] The dependence of refraction on frequencies is shown in Fig. 2 with (a) for the rotational angle of 0° and (b) for 45°, respectively. For better contrast, the data are represented in terms of the average transmission intensity. For the case of $\theta=0°$ shown in Fig. 2(a), the center of the outgoing Gaussian beam is always shifted to the top and positive refraction is observed. For the case of $\theta=45°$ shown in Fig. 2(b), however, due to the large anisotropy, negative refraction could be observed at higher frequencies above 39 kHz, corresponding to the beam center shifting downward. Notice that the refractive angle is dependent on frequencies. Refractive directions with frequencies were also calculated as shown in Figs. 2(a) and 2(b). In the range of scanning frequency from 37 to 43 kHz, the experimental measurements agreed well with the theoretical calculations. At the same frequency, the refractive angle with $\theta=45°$ is always more negative than that with $\theta=0°$. So refractions could be expected to control from positive to negative by rotating the θ from 0° to 45°, a result of the enhancement of the anisotropy.

These observations of different refractions in the cases of $\theta=0°$ and $\theta=45°$ could be well understood by examining the acoustic anisotropic EFS. The corresponding acoustic EFS and its curvature determine the direction of acoustic refraction in SRSC. It is well known that the negative refraction is easier to establish when the anisotropy of EFS is more intense. With rotating θ from 0° to 45°, the scattering sections become larger and the SRSCs EFSs are easier to convex around the M point, corresponding to the more intense anisotropy, so that refractions will change from positive to negative. We also carried out experiments with $\theta=15°$ and 30° to verify our analysis. The results also agreed well with the theoretically calculated relation between the refraction and rotational angle θ shown in Fig. 3(a). The larger θ results in the greater curvature of EFS, and leads to the bigger negative refractive angle. If the frequency is higher, EFSs will change more dramatically so that the refraction's manipulation is more obvious and the scanning range is wider.

Based on negative refractions, a kind of flat lens was also

proposed and established as a superlens to make use of both evanescent waves and propagating waves to produce a real image beyond the diffraction limit.[11–17,20] To further study the effect of the tunable negative refraction, we also calculated the range of the all angle negative refraction (AANR), shown in Fig. 3(b). It is well known that the upper limit of AANR is the frequency with a refractive angle −90° for the incident angle of 90°, while the lower limit is the negative refraction starting frequency for the incident angle very close to 0°.[9] With θ changing from 0° to 45°, however, the lowest band of SRSC is effectively decreased and compressed, resulting in an intense anisotropy. Like negative refraction, AANR is also easily realized by intense anisotropy so that AANR appears at $\theta=27°$ and enlarges with rotating θ to 45°. A tunable acoustic superlens can be constructed by SRSC through such a tunable effect of AANR. When θ is smaller, the minor anisotropy will allow good transmission of acoustic waves, while when θ is larger, the intense anisotropy will create a real image of the acoustic source due to AANR. Of course, waves could also be tuned in the band gap so that they may not transmit. In addition, the tunable effect will be more obvious with a higher filling fraction.[24,25]

An imaging experiment similar to that in Ref. 17 was performed with two different θ of 0° and 45° at 35 kHz, as shown in Fig. 4. To get a point source, the area with most of the emitting transducer was blocked and only left a hole at the center with a diameter of 8 mm (a little bit less than the wavelength). This point source was placed 5 mm in the front of SRSC. By using a 1/4 inch receiver (Brüel & Kjær company, Denmark), all field distributions behind SRSC were measured as shown in Fig. 4. Obviously, a good image was recorded when $\theta=45°$ [Fig. 4(b)] but no image when $\theta=0°$ was recorded [Fig. 4(a)], which is in a good agreement with the theoretical calculation. Wave propagation in the sonic crystal is a kind of multiscattering so that the field pattern is also the accumulation of all scatterings due to the Huygens principle. Hence, some interference patterns occur if waves from different directions satisfy the condition for interference. On the other hand, due to the size of our receiver, which is not much less than the wavelength (but it is very difficult to get a very small transducer within the range of tens of kHz), the resolution of our imaging system is not as good as the theoretical expectation. Ideally, it is possible to get a subwavelength resolution because of the existence of negative refractions.[11–17,20]

In summary, we have experimentally constructed a 2D tunable SRSC with square rods, which results in effective modifications of band structures, then EFS and anisotropy of wave propagations by rotational angles. In this effect, rotating all square rods could change the scattering section in one unit cell, and then manipulate the refraction of the acoustic waves from positive to negative. Based on this tunability, a tunable acoustic AANR superlens could be proposed by SRSC with different rotational angles. The refraction control could also be tuned to a desired frequency range by adjusting the lattice constant and constructing materials of the SRSC, for example, with immersing our structure into liquids such as water.

The tunability we established in SRSC could be applied to control not only the refractions but other features of wave propagations, such as resonant transmission by a defect of sonic crystals. Rotating a rod or an array of rods can easily produce a point defect or a line defect, and even multiple point or line defects. And this idea on SRSC could also be effectively used in the propagation of light, liquid, and other waves, which will lead to great potential in ultrasonics, photoelectronics and so on.

The work was jointly supported by the National 863 High Technology Program, the State Key Program for Basic Research of China, the National Nature Science Foundation of China (Grant No. 50225204), and the program for Changjiang Scholars and Innovative Research Team in University (PCSIRT).

*Email address: yfchen@nju.edu.cn

[1] V. G. Veselago, Sov. Phys. Usp. **10**, 509 (1968).
[2] J. B. Pendry *et al.*, Phys. Rev. Lett. **76**, 4773 (1996).
[3] J. B. Pendry *et al.*, J. Phys.: Condens. Matter **10**, 4785 (1998).
[4] J. B. Pendry *et al.*, IEEE Trans. Microwave Theory Tech. **47**, 2075 (1999).
[5] D. R. Smith *et al.*, Phys. Rev. Lett. **84**, 4184 (2000).
[6] R. A. Shelby *et al.*, Appl. Phys. Lett. **78**, 489 (2001).
[7] R. A. Shelby *et al.*, Science **292**, 77 (2001).
[8] M. Notomi, Phys. Rev. B **62**, 10696 (2000).
[9] E. Cubukcu *et al.*, Nature (London) **423**, 604 (2003).
[10] P. V. Parimi *et al.*, Phys. Rev. Lett. **92**, 127401 (2004).
[11] C. Luo *et al.*, Phys. Rev. B **65**, 201104(R) (2002).
[12] J. B. Pendry, Phys. Rev. Lett. **85**, 3966 (2000).
[13] A. A. Houck *et al.*, Phys. Rev. Lett. **90**, 137401 (2003).
[14] C. Luo *et al.*, Phys. Rev. B **68**, 045115 (2003).
[15] P. V. Parimi *et al.*, Nature (London) **426**, 404 (2003).
[16] X. Zhang and Z. Liu, Appl. Phys. Lett. **85**, 341 (2004).
[17] S. Yang *et al.*, Phys. Rev. Lett. **93**, 024301 (2004).
[18] J. H. Page *et al.*, Phys. Status Solidi B **241**, 3454 (2004).
[19] L. Feng *et al.*, Phys. Rev. B **72**, 033108 (2005).
[20] X. Hu *et al.*, Phys. Rev. E **69**, 030201(R) (2004).
[21] L. Feng *et al.*, J. Appl. Phys. **97**, 073104 (2005).
[22] L. Feng *et al.*, Phys. Rev. B **71**, 195106 (2005).
[23] X. H. Wang *et al.*, Phys. Rev. B **60**, 11417 (1999).
[24] C. Goffaux and J. P. Vigneron, Phys. Rev. B **64**, 075118 (2001).
[25] F. Wu *et al.*, Phys. Rev. E **66**, 046628 (2002).
[26] In order to manufacture a 2D SRSC, an aluminum plate was drilled to be a square array of holes with diameters of 2.3 mm and a lattice constant of 2.5 mm. Holes were arranged as [1, 1] direction with 79 layers in the lateral direction of the plate and 20 layers in the perpendicular direction. The 2D SRSC was constructed by inserting 150 mm long, 1.6 mm wide steel square rods into the periodically drilled plate, and the related parameters are $\rho_{steel}=7800$ kg/m^3, $\rho_{air}=1.21$ kg/m^3, $c_{steel}=6100$ m/s, $c_{air}=334.5$ m/s (sound velocity in air at 0 °C).
[27] M. S. Kushwaha, and B. Djafari-Rouhani, J. Sound Vib. **218**, 697 (1998).